J Eng Math (2007) 59:139–153
DOI 10.1007/s10665-006-9088-4

ORIGINAL PAPER

A nonlinear magnetoelastic tube under extension and inflation in an axial magnetic field: numerical solution

R. Bustamante · A. Dorfmann · R. W. Ogden

Received: 4 April 2006 / Accepted: 2 August 2006 / Published online: 28 September 2006

Abstract In the context of nonlinear magnetoelasticity theory very few boundary-value problems have been solved. The main problem that arises when a magnetic field is present, as compared with the purely elastic situation, is the difficulty of meeting the magnetic boundary conditions for bodies with finite geometry. In general, the extent of the edge effects is unknown a priori, and this makes it difficult to interpret experimental results in relation to the theory. However, it is important to make the connection between theory and experiment in order to develop forms of the magnetoelastic constitutive law that are capable of correlating with the data and can be used for making quantitative predictions. In this paper the basic problem of a circular cylindrical tube of finite length that is deformed by a combination of axial compression (or extension) and radial expansion (or contraction) and then subjected to an axial magnetic field is examined. Such a field cannot be uniform throughout, since the boundary conditions on the ends and the lateral surfaces of the tube would be incompatible in such circumstances. The resulting axisymmetric boundary-value problem is formulated and then solved numerically for the case (for simplicity of illustration) in which the deformation is not altered by the application of the magnetic field. The distribution of the magnetic-field components throughout the body and the surrounding space is determined in order to quantify the extent of the edge effects for both extension and compression of the tube.

Keywords Nonlinear magnetoelasticity · Finite deformations · Magnetoelastic interactions

1 Introduction

Recently, a number of industrial applications that make use of so-called magneto-sensitive (MS) elastomers have been developed. These include controllable membranes, controllable stiffness devices, and applications for the active control of structural components and rapid response interfaces aimed at optimizing the performance of mechanical systems (see, for example, [1,2]). Such applications have great promise since

R. Bustamante · R. W. Ogden (✉)
Department of Mathematics, University of Glasgow, Glasgow G12 8QW, UK
e-mail: rwo@maths.gla.ac.uk

A. Dorfmann
Department of Civil and Environmental Engineering, Tufts University, Medford, MA 02155, USA

MS elastomers rapidly and significantly change their mechanical properties on the application of a magnetic field. There is therefore an increased need for reliable constitutive equations to model the magnetoelastic properties of these materials for use in the analysis and solution of representative boundary-value problems.

We refer to the recent series of papers by Dorfmann and Ogden [3–5] and the references contained therein for the relevant theoretical background based on the general theory of nonlinear magnetoelasticity. These papers also contain solutions to representative boundary-value problems for which exact solutions can be found. For the most part such solutions are idealized in the sense that they apply only to bodies of infinite extent in one or more directions so that edge effects are not present. The purpose of the present paper is to apply the theory, using a prototype choice of model constitutive law, to a boundary-value problem involving finite geometry, for which an exact solution cannot be found. Specifically, we consider as an illustrative problem the extension and inflation of a thick-walled magnetoelastic tube of finite length in the presence of a magnetic field that, remote from the tube, is uniform and in the axial direction. Numerical computation is used to determine the distribution of the magnetic field and the magnetic induction field throughout the body and its exterior, with careful account taken of the boundary conditions on both the ends of the tube and its cylindrical surfaces.

We make use of a particularly simple general formulation for the magnetoelastic interaction, as described by Dorfmann and Ogden [3]. The constitutive equation is based on a modified free-energy function that depends, in addition to the deformation, on the magnetic-field vector as the independent magnetic variable. The relevant magnetic and mechanical balance equations and boundary conditions are summarized in Sect. 2. In Sect. 3, following Dorfmann and Ogden [3], the general constitutive equations for magnetoelastic interactions are given for both compressible and incompressible magnetoelastic materials and then specialized for specific application to incompressible, isotropic magnetoelastic materials.

In Sect. 4, we consider the extension and inflation of a circular cylindrical tube of finite length subject to a magnetic field, which, in the far field, is uniform and parallel to the axial direction of the tube. We remark that, for an infinitely long cylinder, as discussed in [5], the boundary conditions on the cylindrical surfaces can be satisfied exactly in the case of an axial magnetic field that is uniform through the body and the surrounding space since the end conditions do not have an influence. For a finite-length tube, on the other hand, the boundary conditions on the ends of the tube are not compatible with those on the cylindrical surfaces if the field is uniform. Thus, the presence of the body, which is maintained in its circular cylindrical shape by the application of suitable boundary tractions, distorts the originally uniform magnetic field lines in the vicinity of the bounding surfaces, both within and exterior to the body. The resulting boundary-value problem is two-dimensional and is solved using a finite-difference method, with the radial and axial coordinates used as the independent spatial variables. For this purpose we introduce a model constitutive law that can be seen as a prototype for describing the magnetoelastic response of the materials in question. The solution process is reduced to the determination of two scalar potentials, one for the inside of the body and the second for the surrounding vacuum, with appropriate continuity conditions on the bounding interfaces. We determine the spatial distribution of the magnetic field in the deformed configuration throughout the considered space. In particular, the distributions of the radial and axial components of both the magnetic and magnetic-induction fields are shown graphically for the region occupied by the body and its exterior, and the extent of the 'edge' effects is highlighted.

This particular problem is examined for purposes of illustration of the general formulation adopted here, but, of course, the formulation is applicable to any well-posed boundary-value problem and there is no need to restrict attention in general to an axial magnetic field. Our particular choice of problem has the advantage that it represents a feasible experimental set-up and hence affords the possibility of obtaining data to compare directly with the theory.

2 Basic equations

2.1 Kinematics

Consider a magnetoelastic material occupying the reference configuration $\mathcal{B}_0$ when undeformed and in the absence of a magnetic field. Let a material point in $\mathcal{B}_0$ be defined by its position vector $\mathbf{X}$ relative to an arbitrarily chosen origin. When the body is subjected to the deformation $\boldsymbol{\chi}$, the point $\mathbf{X}$ assumes a new position $\mathbf{x} = \boldsymbol{\chi}(\mathbf{X})$ in the resulting deformed configuration, which we denote by $\mathcal{B}$. The deformation gradient tensor $\mathbf{F}$ relative to $\mathcal{B}_0$, and its determinant, are

$$\mathbf{F} = \operatorname{Grad} \boldsymbol{\chi}, \quad J = \det \mathbf{F} > 0, \tag{1}$$

respectively, where Grad is the gradient operator with respect to $\mathbf{X}$ and wherein the notation J is defined.

2.2 Magnetic balance equations

Suppose that the deformed configuration $\mathcal{B}$ arises from the combined application of a magnetic field and boundary tractions. The magnetic-field vector is denoted by $\mathbf{H}$ and the magnetic-induction vector by $\mathbf{B}$. In the absence of material, these are related by the standard equation

$$\mathbf{B} = \mu_0 \mathbf{H}, \tag{2}$$

where μ_0 is the magnetic permeability *in vacuo*. Inside material, on the other hand, the two vectors are connected via a constitutive law, which will be discussed in Sect. 3.

In either case, these vectors satisfy the field equations

$$\operatorname{curl} \mathbf{H} = \mathbf{0}, \quad \operatorname{div} \mathbf{B} = 0, \tag{3}$$

where curl and div, respectively, are the curl and divergence operators with respect to $\mathbf{x}$. We are assuming here that no free currents are present.

Equations 3 are expressed in Eulerian form. Inside a deformed material pull-back operations from $\mathcal{B}$ to $\mathcal{B}_0$ give the corresponding Lagrangian forms of the magnetic field vector, denoted $\mathbf{H}_l$, and magnetic induction vector, denoted by $\mathbf{B}_l$ (see, for example, [3,6,7]). The connections are $\mathbf{H}_l = \mathbf{F}^{\mathrm{T}}\mathbf{H}$ and $\mathbf{B}_l = J\mathbf{F}^{-1}\mathbf{B}$, where $^{\mathrm{T}}$ signifies the transpose (of a second-order tensor). The counterparts of (3) for these vectors are (within the material)

$$\operatorname{Curl} \mathbf{H}_l = \mathbf{0}, \quad \operatorname{Div} \mathbf{B}_l = 0, \tag{4}$$

where Curl and Div, respectively, are the curl and divergence operators with respect to $\mathbf{X}$. Note that it is not meaningful to define $\mathbf{F}$ and hence $\mathbf{H}_l$ and $\mathbf{B}_l$ outside the material.

2.3 Mechanical balance equations

Let ρ_0 and ρ be the mass densities of the material in the reference and deformed configurations, $\mathcal{B}_0$ and $\mathcal{B}$, respectively. Then, recalling that $J = \det \mathbf{F}$, the conservation of mass equation can be written simply as

$$J\rho = \rho_0. \tag{5}$$

The influence of the magnetic field on the mechanical stress in the deforming body may be incorporated through *magnetic body forces* or through a *magnetic stress tensor*. Here, we adopt the latter approach and denote the resulting *total* (Cauchy) stress tensor by $\boldsymbol{\tau}$, which has the advantage of being *symmetric*. In the absence of *mechanical* body forces, the equilibrium equation for a magnetoelastic solid has the (Eulerian) form

$$\operatorname{div} \boldsymbol{\tau} = \mathbf{0}. \tag{6}$$

For more details we refer to, for example, [3,7,8].

As in conventional nonlinear elasticity theory [9], we may define a 'nominal' stress tensor, here denoted $\mathbf{T}$ and referred to as the total nominal stress tensor, which is related to $\boldsymbol{\tau}$ by

$$\mathbf{T} = J\mathbf{F}^{-1}\boldsymbol{\tau}. \tag{7}$$

The equilibrium equation (6) may then be expressed simply in Lagrangian form as

$$\mathrm{Div}\mathbf{T} = \mathbf{0}. \tag{8}$$

2.4 Boundary conditions

At the interfaces between the considered material body and its exterior appropriate boundary conditions must be satisfied by the fields $\mathbf{H}, \mathbf{B}$ and $\boldsymbol{\tau}$. In particular, the vector fields $\mathbf{H}$ and $\mathbf{B}$ satisfy the standard jump conditions

$$\mathbf{n} \times [\![\mathbf{H}]\!] = \mathbf{0}, \quad \mathbf{n} \cdot [\![\mathbf{B}]\!] = 0, \tag{9}$$

where $[\![\cdot]\!]$ signifies a discontinuity across the boundary and $\mathbf{n}$ is its outward unit normal. It is assumed here that there are no surface currents. The boundary condition involving the stress $\boldsymbol{\tau}$, where traction rather than displacement is specified, may be written in the form

$$[\![\boldsymbol{\tau}]\!]\mathbf{n} = \mathbf{0}, \tag{10}$$

and we note that the traction $\boldsymbol{\tau}\mathbf{n}$ on the outer boundary includes a contribution from the (symmetric) Maxwell stress outside the material as well as any mechanical traction applied to the surface of the body. We recall (see, for example, [3]) that the Maxwell stress outside the material, denoted $\boldsymbol{\tau}_{\mathrm{m}}$, is given by

$$\boldsymbol{\tau}_{\mathrm{m}} = \mathbf{H} \otimes \mathbf{B} - \frac{1}{2}(\mathbf{H} \cdot \mathbf{B})\mathbf{I}, \tag{11}$$

where $\mathbf{I}$ is the identity tensor and $\mathbf{B} = \mu_0\mathbf{H}$. Note that the exterior of the body in question is considered to be either a vacuum or a magnetically inactive material.

Equations (9) and (10) may also be expressed in terms of the Lagrangian quantities $\mathbf{H}_l, \mathbf{B}_l$ and $\mathbf{T}$ for the reference counterpart of the discontinuity surface, for details of which we refer to [3].

3 Constitutive equations

In previous papers (for example, [3–5,10]) we considered formulations of the constitutive law based on either $\mathbf{H}_l$, $\mathbf{B}_l$ or the magnetization (not defined here) as the independent magnetic variable. However, for the solution of more specific boundary-value problems it would seem simplest to work with $\mathbf{H}_l$ (or $\mathbf{H}$) since this can be expressed in terms of a scalar potential function. The resulting (coupled) partial differential equations are then equations for this potential and, in the case of an incompressible material, when the deformation is specified (as it is in the problem considered in Sect. 4) the hydrostatic part of the stress.

Thus, in the present paper we consider only a constitutive law with $\mathbf{H}_l$ as the independent magnetic variable and write the 'total' energy function as

$$\Omega^* = \Omega^*(\mathbf{F}, \mathbf{H}_l) \tag{12}$$

in which Ω^* is treated as a function of $\mathbf{F}$ and $\mathbf{H}_l$. The superscript * is retained in order to maintain consistency with the notation used in the papers cited above. Then, for a compressible material, the total nominal stress $\mathbf{T}$ and the magnetic induction $\mathbf{B}_l$ are given by the simple formulas

$$\mathbf{T} = \frac{\partial \Omega^*}{\partial \mathbf{F}}, \quad \mathbf{B}_l = -\frac{\partial \Omega^*}{\partial \mathbf{H}_l}, \tag{13}$$

and for an incompressible material by

$$\mathbf{T} = \frac{\partial \Omega^*}{\partial \mathbf{F}} - p^* \mathbf{F}^{-1}, \quad \mathbf{B}_l = -\frac{\partial \Omega^*}{\partial \mathbf{H}_l}, \tag{14}$$

where p^* is a Lagrange multiplier associated with the incompressibility constraint

$$\det \mathbf{F} = 1. \tag{15}$$

The corresponding Eulerian quantities are given by

$$\boldsymbol{\tau} = J^{-1}\mathbf{F}\frac{\partial \Omega^*}{\partial \mathbf{F}}, \quad \mathbf{B} = -J^{-1}\mathbf{F}\frac{\partial \Omega^*}{\partial \mathbf{H}_l}, \tag{16}$$

and

$$\boldsymbol{\tau} = \mathbf{F}\frac{\partial \Omega^*}{\partial \mathbf{F}} - p^*\mathbf{I}, \quad \mathbf{B} = -\mathbf{F}\frac{\partial \Omega^*}{\partial \mathbf{H}_l} \tag{17}$$

for compressible and incompressible materials, respectively, where $\mathbf{I}$ is again the identity tensor.

3.1 Isotropic magnetoelastic materials

The applied magnetic field introduces a preferred direction in the material analogous to the preferred direction in a transversely isotropic elastic solid. Paralleling the analysis of Spencer [11] for transversely isotropic materials (see also [12,13]), we define an *isotropic* magnetoelastic material as one for which Ω^* is an isotropic function of the two tensors $\mathbf{c}$ and $\mathbf{H}_l \otimes \mathbf{H}_l$, where $\mathbf{c} = \mathbf{F}^{\mathrm{T}}\mathbf{F}$ is the right Cauchy–Green tensor. Here we consider only incompressible materials, for which the principal invariants of $\mathbf{c}$, denoted by I_1 and I_2, are given by

$$I_1 = \operatorname{tr}\mathbf{c}, \quad I_2 = \tfrac{1}{2}\left[(\operatorname{tr}\mathbf{c})^2 - \operatorname{tr}(\mathbf{c}^2)\right], \tag{18}$$

with $I_3 \equiv \det \mathbf{c} = 1$, where tr denotes the trace of a second-order tensor. The additional invariants involving $\mathbf{H}_l$ are denoted (in the notation of [3]) by K_4, K_5, K_6 and are defined by

$$K_4 = |\mathbf{H}_l|^2, \quad K_5 = (\mathbf{c}\mathbf{H}_l)\cdot\mathbf{H}_l, \quad K_6 = (\mathbf{c}^2\mathbf{H}_l)\cdot\mathbf{H}_l. \tag{19}$$

For an incompressible material, Ω^* reduces to a function that depends on these five invariants and we write $\Omega^* = \Omega^*(I_1, I_2, K_4, K_5, K_6)$.

The total stress $\boldsymbol{\tau}$ and the magnetic induction field $\mathbf{B}$ given in (17) now expand out as

$$\boldsymbol{\tau} = 2\Omega_1^*\mathbf{b} + 2\Omega_2^*(I_1\mathbf{b} - \mathbf{b}^2) - p^*\mathbf{I} + 2\Omega_5^*\mathbf{b}\mathbf{H}\otimes\mathbf{b}\mathbf{H} + 2\Omega_6^*(\mathbf{b}\mathbf{H}\otimes\mathbf{b}^2\mathbf{H} + \mathbf{b}^2\mathbf{H}\otimes\mathbf{b}\mathbf{H}), \tag{20}$$

$$\mathbf{B} = -2(\Omega_4^*\mathbf{b}\mathbf{H} + \Omega_5^*\mathbf{b}^2\mathbf{H} + \Omega_6^*\mathbf{b}^3\mathbf{H}), \tag{21}$$

where $\mathbf{b} = \mathbf{F}\mathbf{F}^{\mathrm{T}}$ is the left Cauchy–Green tensor and Ω_i^* is defined as $\partial\Omega^*/\partial I_i$ for $i = 1, 2$, and $\partial\Omega^*/\partial K_i$ for $i = 4, 5, 6$.

In Sect. 4 we apply the above constitutive equations, field equations and boundary conditions in Eulerian form to the problem at hand.

4 Extension and inflation of a cylindrical tube

In a previous paper [5] we considered the extension and inflation of an infinitely long circular cylindrical tube subjected to an axial and a circumferential magnetic field. Solutions for the change in radius as a function of the applied pressure and for the corresponding resultant axial load were given using first the

magnetic induction $\mathbf{B}_l$ and subsequently the magnetic-field vector $\mathbf{H}_l$ as the independent magnetic-field variables.

In this section we again consider the extension and inflation of a cylindrical tube with circular cross-section subjected to an axial magnetic field $\mathbf{H}$, but now for a tube of finite length. Unlike the situation for an infinitely long tube, close to the material boundaries, the magnetic-field lines deviate from the axial direction, essentially because the normal component of $\mathbf{B}$ has to be continuous across the plane ends of the tube, and this boundary condition is not compatible with both the presence of a uniform axial field and the boundary condition that the tangential component of $\mathbf{H}$ has to be continuous across the cylindrical surfaces. As a result, it does not appear possible to find a closed-form analytical solution for the magnetic-field distribution, either inside the body or in the surrounding space. We therefore adopt a numerical scheme to determine the distributions of the magnetic field and magnetic-induction vectors.

4.1 Kinematics

In terms of cylindrical polar coordinates (R, Θ, Z) we describe the undeformed reference configuration of the tube by

$$0 < A \leq R \leq B, \quad 0 \leq \Theta \leq 2\pi \quad 0 \leq Z \leq L, \tag{22}$$

where the interior and exterior radii are denoted by A and B and the total length by L. The tube is deformed by the action of suitable boundary tractions, so that the circular cylindrical shape is maintained. The resulting deformed configuration is then described using cylindrical polar coordinates (r, θ, z) by

$$0 < a \leq r \leq b, \quad 0 \leq \theta \leq 2\pi, \quad 0 \leq z \leq l, \tag{23}$$

where l is the deformed length of the tube and a and b the corresponding inner and outer radii. For an incompressible material, the deformation is given by

$$r = \sqrt{cR^2 + d}, \quad \theta = \Theta, \quad z = \lambda_z Z, \tag{24}$$

where the axial stretch, denoted λ_z, is constant, $c = \lambda_z^{-1}$ and d is a constant $(= a^2 - cA^2)$.

The deformation-gradient tensor $\mathbf{F}$, with respect to the polar coordinate axes, then has component matrix, here denoted F, in cylindrical coordinates given by

$$\mathsf{F} = \mathrm{diag}\,[\lambda^{-1}\lambda_z^{-1}, \lambda, \lambda_z], \tag{25}$$

in which λ is defined as $\lambda = r/R$. The diagonal entries are just the principal stretches

$$\lambda_1 = \lambda^{-1}\lambda_z^{-1}, \quad \lambda_2 = \lambda \equiv \frac{r}{R}, \quad \lambda_3 = \lambda_z, \tag{26}$$

which satisfy the incompressibility condition (15) in the form $\lambda_1\lambda_2\lambda_3 = 1$.

4.2 The field equations

The considered problem is axisymmetric when a magnetic field is applied that is axial and uniform far from the tube. Thus, in the deformed configuration, there is no dependence on θ, and the magnetic-field vectors and the stress tensor depend on both the radius r and the axial coordinate z, i.e., $\mathbf{B} = \mathbf{B}(r, z)$, $\mathbf{H} = \mathbf{H}(r, z)$, and $\boldsymbol{\tau} = \boldsymbol{\tau}(r, z)$. Note that, in general, when the magnetic field is applied to a circular cylindrical tube, when deformed as described in the above section, it will deform further and into a configuration in which the deformation depends on z as well as r unless appropriate stresses are applied to maintain the shape. Here we assume that such stresses are applied so that the deformation is known explicitly. The problem involving a more general axisymmetric deformation will be considered elsewhere.

For the numerical calculation we shall work in terms of the Eulerian forms of the field equations, which we summarize here as

$$\operatorname{curl}\mathbf{H} = \mathbf{0}, \quad \operatorname{div}\mathbf{B} = 0, \quad \operatorname{div}\boldsymbol{\tau} = \mathbf{0}. \tag{27}$$

From the first equation in (27) we deduce the existence of a scalar (magnetic) potential function φ such that

$$\mathbf{H} = -\operatorname{grad}\varphi, \tag{28}$$

which applies both within and outside the material, and we note in passing that $\mathbf{H}_l = \mathbf{F}^{\mathrm{T}}\mathbf{H} = -\operatorname{Grad}\varphi$.

Now, *outside* the body, where we assume that $\mathbf{B} = \mu_0\mathbf{H}$, as in vacuum or in a material with no magnetization, we have $\operatorname{div}\mathbf{H} = 0$ and (28) yields Laplace's equation

$$\nabla^2\varphi = 0 \tag{29}$$

for the potential φ.

On the other hand, *inside* the material the magnetic induction is determined by the constitutive law (21), which for convenience we write compactly as

$$\mathbf{B} = -\boldsymbol{\mathcal{C}}\mathbf{H} \equiv \boldsymbol{\mathcal{C}}\operatorname{grad}\varphi, \tag{30}$$

where $\boldsymbol{\mathcal{C}}$ is defined as

$$\boldsymbol{\mathcal{C}} = 2(\Omega_4^*\mathbf{b} + \Omega_5^*\mathbf{b}^2 + \Omega_6^*\mathbf{b}^3), \tag{31}$$

which depends on $\operatorname{grad}\varphi$ as well as the deformation.

Since, inside the material, we again have the field equation $\operatorname{div}\mathbf{B} = 0$ then, instead of (29), we have the equation

$$\operatorname{div}(\boldsymbol{\mathcal{C}}\operatorname{grad}\varphi) = 0 \tag{32}$$

inside the material. The potential φ can be taken as continuous across the interfaces, so that we do not use separate notations for it within and outside the material. For an energy function Ω^* and for a known deformation $\mathbf{b} = \mathbf{F}\mathbf{F}^{\mathrm{T}}$, Eqs. (29) and (32) can in principle be solved for the scalar potential φ subject to the boundary conditions (9) applied to the interfaces. As a consequence, the spatial distributions of the fields $\mathbf{H}$ and $\mathbf{B}$ and the stress distribution can be determined.

We now turn briefly to the equilibrium equation $(27)_3$. For the considered deformation it is easy to show from (20) that $\tau_{r\theta} = \tau_{\theta z} = 0$ and that $(27)_3$ reduces to the two component equations

$$\frac{\partial\tau_{rr}}{\partial r} + \frac{\partial\tau_{rz}}{\partial z} + \frac{1}{r}(\tau_{rr} - \tau_{\theta\theta}) = 0, \quad \frac{\partial\tau_{rz}}{\partial r} + \frac{\partial\tau_{zz}}{\partial z} + \frac{1}{r}\tau_{rz} = 0. \tag{33}$$

Since the normal components τ_{rr} and τ_{zz} involve the Lagrange multiplier p^* these two equation essentially determine p^* as a function of r and z and hence the distribution of stress and the mechanical boundary tractions required to maintain the deformation. We do not therefore consider these equations further.

4.3 Boundary conditions

Let the magnetic far-field boundary condition for this problem be given as a constant axial magnetic field with nonzero component H_0, i.e., the applied field is parallel to the axis of the tube, as depicted in Fig. 1. Due to interaction with the body, the magnetic field lines deviate from the axial direction near the boundaries so as to satisfy the continuity conditions specified in (9), and the field will therefore depend on both coordinates r and z.

A circular cylindrical tube subjected to axial extension and inflation maintains its original axisymmetric configuration provided suitable boundary tractions are applied. The numerical solution can therefore be

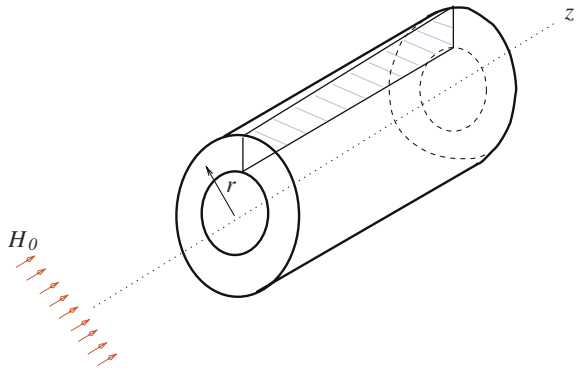

Fig. 1 The three-dimensional problem of a deformed circular cylindrical tube in an axial magnetic far field

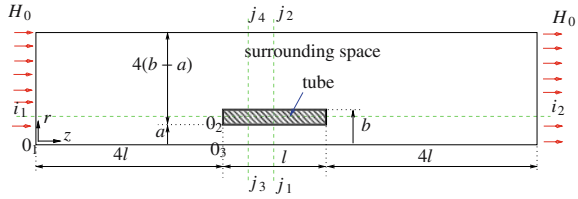

Fig. 2 A section through the axis of the tube and its exterior corresponding to the domain of numerical computation in terms of coordinates (r, z)

reduced to a two-dimensional problem restricted to the r–z-plane, as illustrated in Fig. 2. For the given deformation, determination of the magnetic field distribution reduces firstly to defining a particular form of the energy function Ω^* in terms of the invariants I_1, I_2, K_4, K_5, K_6 and secondly to finding a solution of Eq. (32) for the scalar potential φ for points inside the body. In the surrounding space, the solution of the Laplace equation (29) determines φ.

The continuity condition on the material interfaces given by the equation $\mathbf{n} \times [\![\mathbf{H}]\!] = \mathbf{0}$ is satisfied automatically, since φ may be taken as continuous across these boundaries, as noted earlier. The continuity condition $[\![\mathbf{B}]\!] \cdot \mathbf{n} = 0$ requires that the radial component B_r is continuous across $r = a$ and $r = b$ and that the axial component B_z is continuous across the ends of the tube $z = 0$ and $z = l$ (here z is measured relative to the origin 0_3 in Fig. 2).

4.4 Illustration

Solutions of (29) and (32) are needed in order to determine the magnetic-field distributions inside the material and in the surrounding space. In terms of the cylindrical coordinates r and z, Eq. (29) has the form

$$\frac{\partial^2 \varphi}{\partial r^2} + \frac{1}{r}\frac{\partial \varphi}{\partial r} + \frac{\partial^2 \varphi}{\partial z^2} = 0, \tag{34}$$

and Eq. (32) becomes

$$\left(\frac{\mathcal{C}_{rr}}{r} + \frac{\partial \mathcal{C}_{rr}}{\partial r}\right)\frac{\partial \varphi}{\partial r} + \mathcal{C}_{rr}\frac{\partial^2 \varphi}{\partial r^2} + \frac{\partial \mathcal{C}_{zz}}{\partial z}\frac{\partial \varphi}{\partial z} + \mathcal{C}_{zz}\frac{\partial^2 \varphi}{\partial z^2} = 0, \tag{35}$$

where $\mathcal{C}_{rr} = \mathcal{C}_{rr}(r, z)$ and $\mathcal{C}_{zz} = \mathcal{C}_{zz}(r, z)$ are the radial and axial normal components of $\boldsymbol{\mathcal{C}}$. For purposes of numerical computation it is necessary to restrict attention to a finite region. We therefore choose a computational grid whose dimensions are nine times the length of the tube in the axial direction and five times the inner radius (of the tube) in the radial direction, and, for definiteness, we set $b = 2a$ (see Fig. 2). Different choices do not affect the results significantly.

In general, extensive experimental test data are required to develop specific forms of Ω^* in order to correlate data with the solution of this problem. Such data are not currently available for the considered problem, although some data from uniaxial traction and simple shear experiments have recently been produced (see, for example, [14–18]). In the absence of suitable data, we introduce a specific prototype form of Ω^* that reflects the behaviour observed in the limited experiment data on magnetoelastic elastomers available in the literature.

For purposes of illustration we consider a simplified form of Ω^* that depends only on I_1 and K_4. Then, the stress (20) and magnetic induction (21) reduce to

$$\boldsymbol{\tau} = 2\Omega_1^*\mathbf{b} - p^*\mathbf{I}, \quad \mathbf{B} = -2\Omega_4^*\mathbf{b}\mathbf{H}, \tag{36}$$

respectively, with $\mathbf{H} = -\text{grad}\,\varphi$. We also define a dimensionless form of K_4, namely $\bar{K}_4 = K_4/\kappa$, where κ is a constant that enables a suitable scaling to be made in order to produce the appropriate relative magnitudes of the mechanical and magnetic effects.

To be more specific, we now consider the form of Ω^* given by

$$\Omega^* = \frac{1}{k}\left[\alpha_0 + \beta_0 \tanh\left(\bar{K}_4^n\right)\right]\left[\frac{(I_1-1)^k}{2^k} - 1\right] + \nu\left(\bar{K}_4\right), \tag{37}$$

where α_0, β_0, n and k are positive constants, with $n \geq 1, k \geq 1/2$. (Note that α_0 corresponds to the shear modulus of the underlying elastic material in the absence of magnetic effects.) The form of (37) is motivated by an elastic strain–energy function that has been used to solve a number of specific boundary-value problems (see, for example, [19]) and reduces to it in the absence of a magnetic field provided we take $\nu(0) = 0$. When there is no deformation, the first term vanishes, which allows the remaining term involving the function ν to be interpreted as the magnetic energy in the undeformed configuration (in which there is a residual stress due to the presence of the magnetic field).

It is convenient to assume a form for ν such that $\nu'(\bar{K}_4)$ is given by

$$\nu'\left(\bar{K}_4\right) = -\kappa\gamma_0\bar{K}_4^{n-1}\,\text{sech}^2\left(\bar{K}_4^n\right) + \kappa\delta_0\tanh\left(\bar{K}_4^2\right) - \kappa\varepsilon_0, \tag{38}$$

where γ_0, δ_0 and ε_0 are constants. An explicit expression for the function ν can be obtained by integrating (38) but is not needed here.

In the expressions (36) we require the explicit forms of Ω_1^* and Ω_4^*, which are

$$\Omega_1^* = \left[\alpha_0 + \beta_0\tanh\left(\bar{K}_4^n\right)\right]\frac{(I_1-1)^{k-1}}{2^k}, \tag{39}$$

$$\Omega_4^* = \frac{n\beta_0}{k\kappa}\bar{K}_4^{n-1}\,\text{sech}^2\left(\bar{K}_4^n\right)\left[\frac{(I_1-1)^k}{2^k} - 1\right] - \gamma_0\bar{K}_4^{n-1}\,\text{sech}^2\left(\bar{K}_4^n\right) + \delta_0\tanh\left(\bar{K}_4^2\right) - \varepsilon_0. \tag{40}$$

These equations provide the nonlinear dependences of Ω_1^* and Ω_4^* on K_4, which are illustrated in the Fig. 3.

The choice of the dependence of Ω^* given in (37) on $\bar{K}_4$ is motivated by reference to the phenomenon of magnetic saturation that arises for magnetic fields of sufficient strength, as we now discuss. First we note that for a magnetoelastic material with negligible magnetization, the magnetic induction in the undeformed configuration is given approximately by $\mathbf{B} = \mu_0\mathbf{H}$, while from $(36)_2$ we have $\mathbf{B} = -2\Omega_4^*\mathbf{H}$. Thus, for very small magnetization and infinitesimal deformation, the numerical value of $-2\Omega_4^*$ should approach the value of the permeability μ_0. On the other hand, for an increasing magnetic field, the material reaches magnetic saturation and Ω_4^* approaches a limiting value that is independent of K_4, as illustrated in Fig. 3. The precise nature of the dependence of Ω_1^* and Ω_4^* on K_4 remains to be determined when sufficient data become available. In Fig. 3, Ω_1^* (left-hand figure) and Ω_4^* (right-hand figure) are each plotted against K_4 for three different values of I_1, specifically $I_1 = 3.1027, 3.3, 3.5$. The first of these arises as the smallest value of I_1 through the wall in the numerical solution of the problem, while the other two values are chosen to

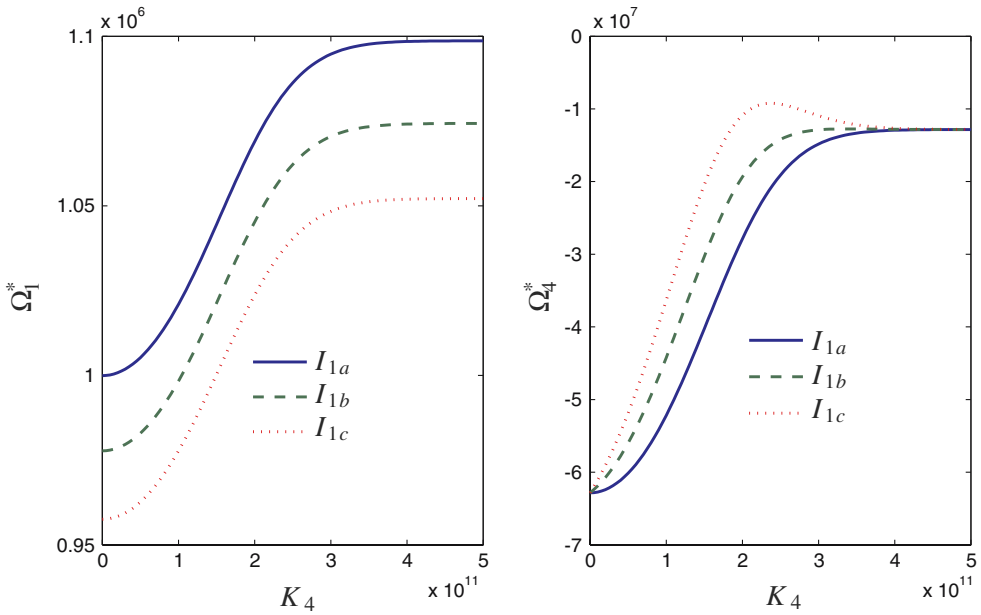

Fig. 3 The nonlinear dependence of Ω_1^* (left figure) and Ω_4^* (right figure) on K_4 (which has units [Amp^2/m^2]) for $I_1 = 3.1027\,(I_{1a}), 3.3\,(I_{1b}), 3.5\,(I_{1c})$

Table 1 Numerical values for the parameters used in the energy function

α_0	2.025 [MPa]
β_0	0.2 [MPa]
γ_0	9.49344×10^{-8} [N/Amp^2]
δ_0	5×10^{-7} [N/Amp^2]
ε_0	$2\pi\times10^{-7}$ [N/Amp^2]
κ	2.15×10^{11} [Amp^2/m^2]
k	3/4
n	2

illustrate the dependence on the deformation. For the solution of the considered boundary-value problem we use, for simplicity, the dependence given by Eqs. (39) and (40), as reflected in Fig. 3. The values of the different constants that appear in (39) and (40) are given in Table 1. Note, in particular, that $\varepsilon_0 = \mu_0/2$.

In the next subsection, the numerical results obtained for the spatial distribution of the magnitudes of the magnetic field and magnetic induction are summarized. To solve (34) and (35) a finite-difference method is used, with the required boundary conditions enforced by using a recurrence algorithm. Different aspect ratios of the cylindrical tube are considered: specifically, we use aspect ratios $l/a = 4, 6, 8$ and describe the deformation through the constants c and d introduced in Eq. (24). Axial compression (extension) corresponds to $c > 1\,(<1)$, and we consider values $c = 0.5, 1, 1.2, 2$ with $d = 0$ or 0.0002 (in the latter d is nondimensionalized by choosing units so that $A = 1$). The magnetic-field distributions inside the tube wall in the undeformed configuration are compared with those in the deformed configurations. For each calculation we set $b = 2a$, so that the wall thickness of the tube is a, as shown in Fig. 2. Note that for $d = 0$ the deformation is homogeneous, while for $d \neq 0$ the deformation is nonhomogeneous since λ then depends on r.

4.5 Results

Let the applied magnetic field be parallel to the axial direction of the circular tube at 'infinity'. The field is distorted by the presence of the magnetoelastic solid and a radial component of the field is generated in the neighbourhood of the material boundaries, both outside and inside the material.

Figure 4 shows the dimensionless magnitude of the axial component of the magnetic field through the material wall for an arbitrary (r, z) plane and for aspect ratio $l/a = 4$. For this illustration the values $c = 1.2$ and $d = 0.0002$ were chosen. The origin of the nondimensionalized coordinate system in Fig. 4 is indicated by 0_2 in Fig. 2, so that r/a and z/l both run from 0 to 1. The results show that the magnetic field is essentially constant away from the boundary and symmetric about the centre $z/l = 0.5$ of the tube. Similarly, for the same geometry and deformation, the dimensionless magnitude of the radial component of the magnetic field is shown in Fig. 5, which reveals that the radial component is antisymmetric with respect to $z/l = 0.5$ and $r/a = 0.5$. In each case the magnetic field is nondimensionalized with respect to the far field H_0, which is given the value 10^5 Amp/m.

The magnitudes of the axial and radial components of the magnetic field within the material depend on the aspect ratio l/a of the tube. The distribution of these values along the line $\overline{i_1 i_2}$ identified in Fig. 2 is shown in Fig. 6 for aspect ratios $l/a = 4, 6, 8$. The line $\overline{i_1 i_2}$ is located at a distance of $3a/2$ from the centreline shown in Fig. 2. The magnitude of the axial component shows a greater dependence on the aspect ratio than the radial component. The extent of the 'edge' effects and nonuniformity of the axial magnetic field is apparent, while the radial component of the field is relatively small.

Variations in the magnitudes of the dimensionless axial and radial components of the magnetic field in the radial direction at two different axial locations are shown in Fig. 7 for aspect ratios of $l/a = 4, 6, 8$. Two significant locations are considered, at $z/l = 0.5$ and $z/l = 0.25$, which are indicated, respectively, by the lines $\overline{j_1 j_2}$ and $\overline{j_3 j_4}$ in Fig. 2. It is interesting to note that in each case the radial component of the magnetic field vanishes on the centre line $z/l = 0.5$, as expected from the antisymmetric distribution shown previously in Fig. 5. In Figs. 6 and 7 the values $c = 1.2$ and $d = 0.0002$ were again used.

Figure 8 shows the variation of the axial and radial components along the line $\overline{i_1 i_2}$ when the tube is undeformed ($c = 1$, $d = 0$) or subjected to the deformation corresponding to the parameters $c = 0.5$ (extension), $c = 2$ (compression), with $d = 0.0002$ in each case. An aspect ratio of $l/a = 4$ is used here. Extension of the tube has, in particular, a tendency to make the axial field more uniform while

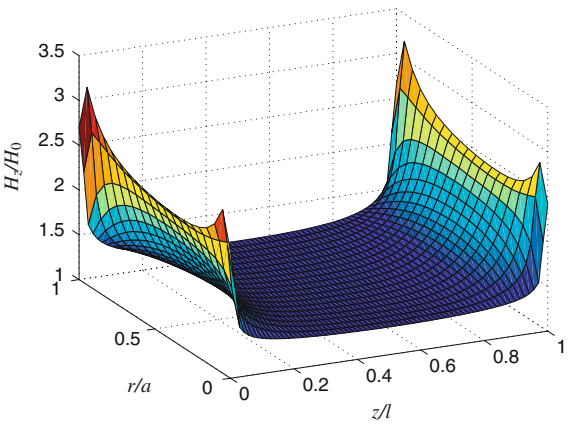

Fig. 4 Magnitude of the dimensionless axial component of the magnetic field through the tube wall in an arbitrary (r, z) plane for aspect ratio $l/a = 4$, for a tube under compression ($c = 1.2$) with $d = 0.0002$

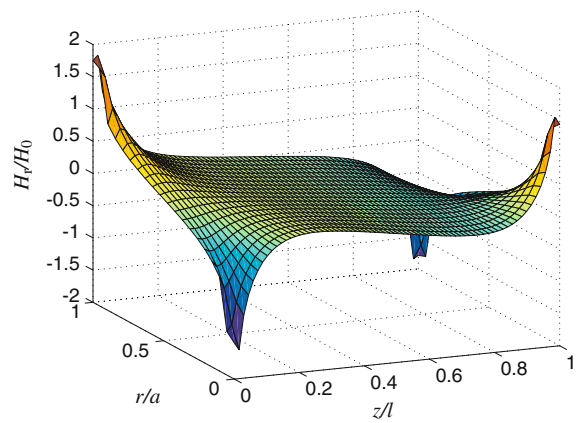

Fig. 5 Magnitude of the dimensionless radial component of the magnetic field inside the material wall on an arbitrary (r, z) plane for aspect ratio $l/a = 4$, for a tube under compression ($c = 1.2$) with $d = 0.0002$

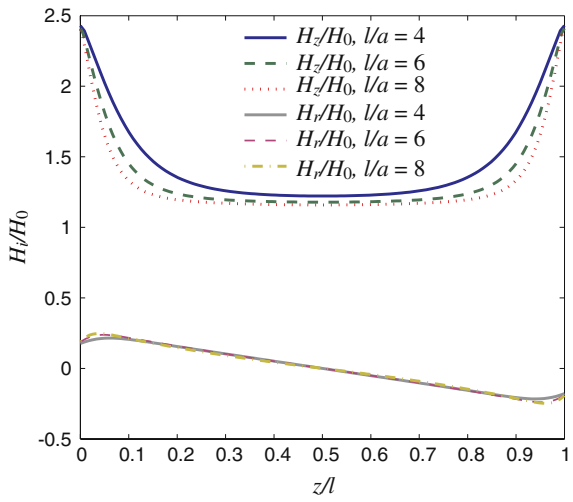

Fig. 6 Magnitudes of the dimensionless axial and radial components of the magnetic field H_i/H_0, $i = r, z$, along the axial direction for aspect ratios $l/a = 4, 6, 8$ and at radial location $\overline{i_1 i_2}$ in Fig. 2, for $c = 1.2$ and $d = 0.0002$

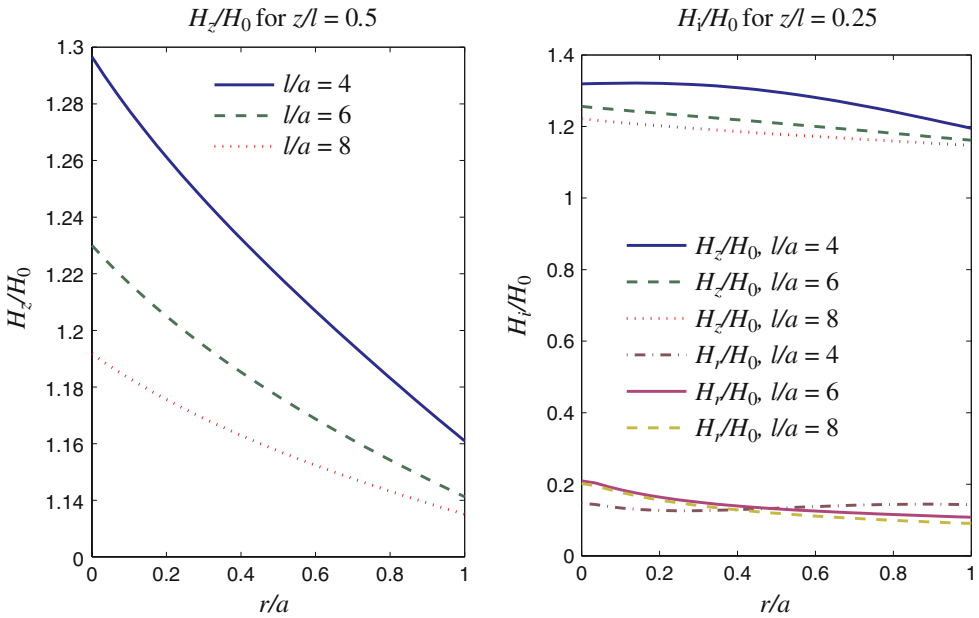

Fig. 7 Dependence of the magnitudes of the dimensionless axial and radial components of the magnetic field H_i/H_0, $i = r, z$, on the dimensionless radius at two different axial locations and for aspect ratios $l/a = 4, 6, 8$ and for $c = 1.2$ and $d = 0.0002$

compression has the opposite effect. Similarly, the variations of the same components along the radial direction, located at $z/l = 0.25$ and indicated by $\overline{j_3 j_4}$ in Fig. 2, are shown in Fig. 9 for the undeformed and deformed configurations. In this case no clear pattern in the relative effects of extension and compression is evident.

In Fig. 10, at the radial station corresponding to the line $\overline{i_1 i_2}$ in Fig. 2, the axial component B_z and the radial component H_r are plotted in dimensionless forms (respectively B_z/B_0 and H_r/H_0, with $B_0 = \mu_0 H_0$) for the whole axial range of the computation (with z/l running from 0 to 9) in order to illustrate the continuity of the axial component of the magnetic induction **B** and the radial component of the magnetic field **H**. The component B_z is continuous on the ends of the tube (located at $z/l = 4, 5$). This is clearly shown in the upper graph of Fig. 10 for aspect ratios of $l/a = 4, 6$ and 8. Outside the material, the magnetic

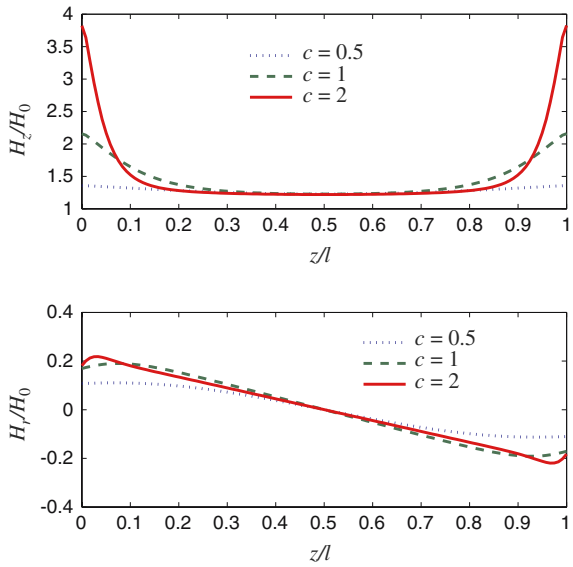

Fig. 8 Variation of the dimensionless axial and radial components of the magnetic field for $l/a = 4$ along the axial direction $\overline{i_1 i_2}$ ($r/a = 3/2$) for the undeformed configuration ($c = 1$, and $d = 0$) and two deformed configurations corresponding to $c = 0.5$ and $c = 2$ (with $d = 0.0002$)

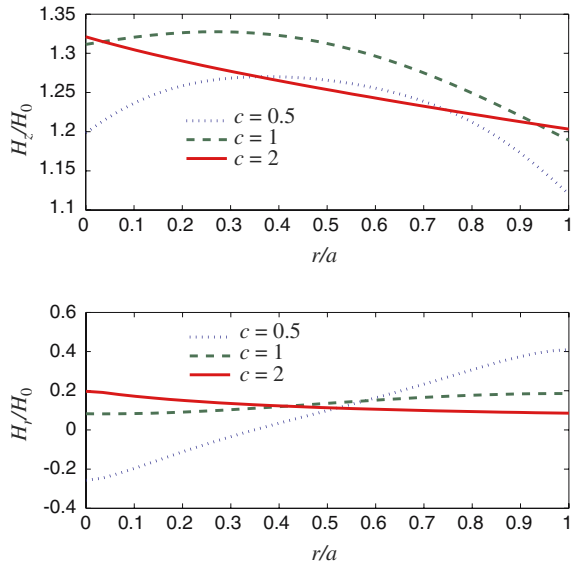

Fig. 9 Variation of the axial and radial components of the magnetic field for $l/a = 4$ along the radial direction at axial location $z/l = 0.25$ (line $\overline{j_3 j_4}$) for the undeformed configuration ($c = 1$, and $d = 0$) and two deformed configurations corresponding to $c = 0.5$ and $c = 2$ (with $d = 0.0002$)

induction is obtained from the applied magnetic field by application of the standard equation $\mathbf{B} = \mu_0 \mathbf{H}$. The continuity of the radial component H_r of the magnetic field on the same boundaries is illustrated in the lower graph in Fig. 10. Also, outside the material and sufficiently far from the tube the magnetic field reduces to a field with an axial component only, i.e., the radial component vanishes. For these computations the values $c = 1.2$ and $d = 0.0002$ were used.

Figure 11 shows the dimensionless radial component of the magnetic induction and the axial component of the magnetic field for aspect ratios of 4, 6 and 8 along the line $\overline{j_3 j_4}$ located at $z/l = 0.25$ (relative to the origin 0_2 in Fig. 2). The cylindrical boundaries correspond to $r/a = 1, 2$. Note, that the radial component of the magnetic induction vanishes on the tube axis, as expected. As in Fig. 10 the values $c = 1.2$ and $d = 0.0002$ were used for the calculations.

5 Closing remarks

In this paper we have obtained illustrative numerical solutions of Eq. (35) for the body and of Laplace's equation (34) for its exterior using the continuity conditions (9). This is the first time in the nonlinear context, as far as we are aware, that full account has been taken of the boundary conditions in order to quantify the extent of the edge effects associated with the finite geometry. The constitutive model that we have introduced is a prototype model in that it represents a first attempt towards the development of constitutive models that can be correlated with experimental data as such data become available.

For problems with finite geometry such as that considered here it is clear that closed form analytic solutions cannot be found and numerical solution is necessary. For more complex geometries it will be appropriate to use a finite-element framework for the solution of more general boundary-value problems. Such a framework is currently being developed. This approach inevitably requires consideration of ques-

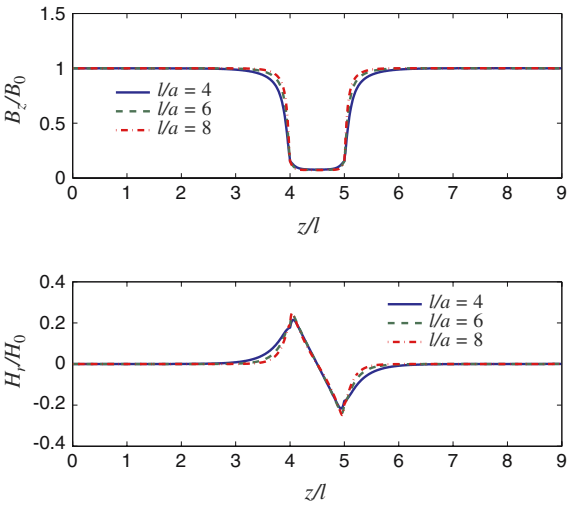

Fig. 10 Illustration of the continuity of the dimensionless axial component of the magnetic induction **B** and of the radial component of the dimensionless magnetic field **H** for $l/a = 4, 6, 8$ with $c = 1.2$ and $d = 0.0002$ at radial location corresponding to the line $\overline{i_1 i_2}$ in Fig. 2. The material is located in the interval $z/l = [4, 5]$

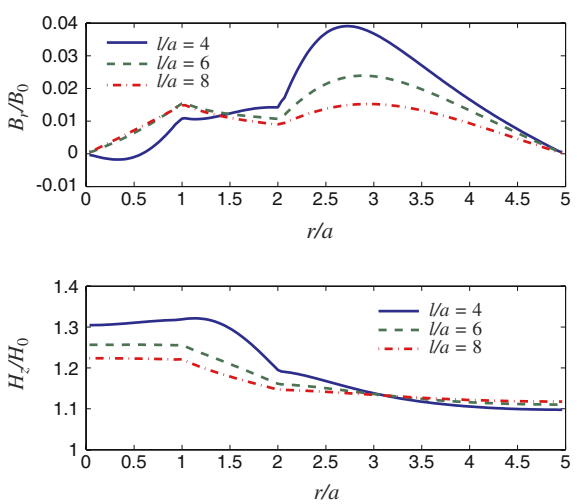

Fig. 11 Variation of the radial component of the dimensionless magnetic induction and the axial component of the dimensionless magnetic field for aspect ratios $l/a = 4, 6, 8$ with $c = 1.2$ and $d = 0.0002$ along the radial line $\overline{j_3 j_4}$ in Fig. 2. The material is located in the interval $r/a = [1, 2]$

tions such as convexity of the energy function and aspects of stability. Some discussion of this is contained in the paper by Kankanala and Triantafyllidis [8], but a more detailed treatment of these aspects is needed.

Finally, we have assumed here that the considered magnetoelastic material is isotropic. However, the magnetoelastic effects seem to be enhanced if the magnetic particles are distributed in an elastomer during the curing process *in the presence of a magnetic field* (see, for example, [18]). Under such conditions the particles are aligned by the magnetic field and generate a preferred direction in the material, so that it is no longer isotropic. This requires a more general form of constitutive law, details of which will be reported in a separate communication.

Acknowledgements The work of RB is supported by the University of Glasgow and by a UK ORS award.

References

1. Jolly MR, Carlson JD, Muñoz BC (1996) A model of the behaviour of magnetorheological materials. Smart Mater Struct 5:607–614
2. Farshad M, Le Roux M (2004) A new active noise abatement barrier system. Polym Test 23:855–860
3. Dorfmann A, Ogden RW (2004) Nonlinear magnetoelastic deformations. Quart J Mech Appl Math 57:599–622
4. Ogden RW, Dorfmann A (2005) Magnetomechanical interactions in magneto-sensitive elastomers. In: Austrell P-E, Kari L (eds) Proceedings of the third European conference on constitutive models for rubber, Stockholm, June 2005. Balkema, Rotterdam, pp 531–543
5. Dorfmann A, Ogden RW (2005) Some problems in nonlinear magnetoelasticity. ZAMP 56:718–745
6. Dorfmann A, Ogden RW (2003) Nonlinear magnetoelastic deformations of elastomers. Acta Mech 167:13–28
7. Steigmann DJ (2004) Equilibrium theory for magnetic elastomers and magnetoelastic membranes. Int J Non-Linear Mech 39:1193–1216
8. Kankanala SV, Triantafyllidis N (2004) On finitely strained magnetorheological elastomers. J Mech Phys Solids 52:2869–2908
9. Ogden RW (1997) Non-linear elastic deformations. Dover, New York
10. Bustamante R, Dorfmann A, Ogden RW (2006) Universal relations in isotropic nonlinear magnetoelasticity. Quart J Mech Appl Math, 59: 435–450

11. Spencer AJM (1971) Theory of invariants. In: Eringen AC (ed) Continuum physics, vol 1. Academic Press, New York, pp 239–353
12. Holzapfel GA (2000) Nonlinear solid mechanics. A continuum approach for engineering. Wiley, Chichester
13. Ogden RW (2001) Elements of the theory of finite elasticity. In: Fu YB, Ogden RW (eds) Nonlinear elasticity: theory and applications, London Mathematical Society, Lecture notes vol 283. Cambridge University Press, Cambridge, pp 1–57
14. Ginder JM, Nichols ME, Elie LD, Tardiff JL (1999) Magnetorheological elastomers: properties and applications. In: Bar-Cohen J (ed) Proceedings of SPIE, vol 3675, Smart structures and materials. SPIE Press, pp 131–138
15. Bossis G, Abbo C, Cutillas S, Lacis S, Métayer C (2001) Electroactive and electrostructured elastomers. Int J Modern Phys B 15:564–573
16. Bellan C, Bossis G (2002) Field dependence of viscoelastic properties of MR elastomers. Int J Modern Phys B 16:2447–2453
17. Varga Z, Filipcsei G, Szilággi A, Zrínyi M (2005) Electric and magnetic field-structured smart composited. Macromol Symp 227:123–133
18. Varga Z, Filipcsei G, Zrínyi M (2006) Magnetic field sensitive functional elastomers with timeable modulus. Polymer 47:227–233
19. Jiang X, Ogden RW (1998) On azimuthal shear of a circular cylindrical tube of compressible elastic material. Quart J Mech Appl Math 51:143–158